

# Studying Two-body Nonleptonic Weak Decays of Hyperons with Topological Diagram Approach

Yuan-Guo Xu<sup>1,†</sup>, Xiao-Dong Cheng<sup>2,‡</sup>, Jie-Lei Zhang<sup>2,§</sup> and Ru-Min Wang<sup>1,§</sup>

<sup>1</sup>College of Physics and Communication Electronics, JiangXi Normal University, NanChang, JiangXi 330022, China

<sup>2</sup>College of Physics and Electronic Engineering, XinYang Normal University, XinYang, Henan 464000, China

<sup>†</sup>yuanguoxv@163.com

<sup>‡</sup>chengxd@mails.ccnu.edu.cn

<sup>§</sup>zhangjielei@ihep.ac.cn

<sup>§</sup>ruminwang@sina.com

Many decays of light baryons consisting of light  $u, d, s$  quarks have been measured, and these decays could be used to test the approach with SU(3) flavor symmetry. We study two-body nonleptonic weak decays of light baryon octet ( $T_8$ ) and baryon decuplet ( $T_{10}$ ) by the topological diagram approach in this work. For  $T_{10} \rightarrow T_8 P_8$  ( $P_8$  is the light pseudoscalar meson octet) decays, we find that all relevant not-yet-measured branching ratios have been predicted by using three experimental data of  $\mathcal{B}(\Omega^- \rightarrow \Xi^0 \pi^-, \Xi^- \pi^0, \Lambda^0 K^-)$ . For  $T_{10} \rightarrow T'_{10} P_8$  decays, we obtain the decay amplitudes and the amplitude relations by both the topological diagram approach and the SU(3) irreducible representation approach, and get  $\mathcal{B}(\Xi^{*0} \rightarrow \Sigma^{*+} \pi^-) < 2.1 \times 10^{-15}$  and  $\mathcal{B}(\Xi^{*-} \rightarrow \Sigma^{*0} \pi^-) < 1.5 \times 10^{-15}$  by the 90% CL experimental upper limit of  $\mathcal{B}(\Omega^- \rightarrow \Xi^{*0} \pi^-)$ .  $T_8 \rightarrow T'_8 P_8$  decays are quite complex, and we find that W-exchange diagrams give large and even dominant contributions by using the experimental data and the isospin relations.

## I. INTRODUCTION

Many two-body nonleptonic weak decays of the octet and decuplet baryons (such as  $\Sigma^+ \rightarrow p \pi^0$ ,  $\Sigma^+ \rightarrow n \pi^+$ ,  $\Sigma^- \rightarrow n \pi^-$ ,  $\Lambda^0 \rightarrow p \pi^-$ ,  $\Lambda^0 \rightarrow n \pi^0$ ,  $\Xi^- \rightarrow \Lambda^0 \pi^-$ ,  $\Xi^0 \rightarrow \Lambda^0 \pi^0$ ,  $\Omega^- \rightarrow \Xi^0 \pi^-$ ,  $\Xi^- \pi^0$ ,  $\Lambda^0 K^-$ ) were measured a long time ago by SPEC, HBC, OSPK etc [1]. Now the sensitivity for measurements of  $\Lambda, \Sigma, \Xi, \Omega$  hyperon decays is in the range of  $10^{-5} - 10^{-8}$  at the BESIII [2–5], and these hyperons are also produced copiously at the LHCb experiment [6, 7]. The precise measurements from the BESIII and LHCb experiments will confirm the earlier experimental data from SPEC, HBC, OSPK etc, and will give new information about determining the V-A structure and quark-flavor mixing [8–10] as well as probing the non-standard charged current interactions [11, 12].

In the theoretical side, the heavy quark expansion can not be used in the light baryons decays, so the factorization does not work well. There is no reliable method to calculate these decay matrix elements at present. In the lack of reliable calculations, some model-independent approaches can provide very useful information about the decays, such as SU(3)/U(3) flavor symmetry (see for instance Refs. [13–29]) and flavor topological diagram approach (TPA) (see for instance Refs. [30–44]). These approaches are independent of the detailed dynamics, and offer an opportunity to relate different decay modes. The decay matrix elements are directly extracted from the experimental data, despite of their unclear sources. In the TPA, decay amplitudes are represented by connecting quark line flows in different ways and then relate them by the SU(3) symmetry. Therefore, the TPA gives a better understanding of dynamics in the different amplitudes.

In this paper, we will use the TPA to study  $T_{10} \rightarrow T_8 M_8$ ,  $T_{10} \rightarrow T'_{10} M_8$  and  $T_8 \rightarrow T'_8 M_8$  two-body nonleptonic

weak decays. We will firstly construct the TPA amplitudes for different kinds of  $T_8$  and  $T_{10}$  nonleptonic decays, secondly obtain the decay amplitude relations between different decay modes, then extract the TPA amplitudes from the available data, and finally analyze the size of the different kinds of contributions or predict the not-yet-measured modes for further tests in experiments.

This paper is organized as follows. In Sec. II, we give the effective Hamiltonian for nonleptonic  $s \rightarrow u\bar{u}d$  process and the expression of the branching ratios. In Sec. III, we firstly give the TPA amplitudes and then give our numerical results and analysis for  $T_{10} \rightarrow T_8 M_8$ ,  $T_{10} \rightarrow T'_{10} M_8$  and  $T_8 \rightarrow T'_8 M_8$  decays. Section IV contains our summary and conclusion.

## II. Theoretical framework

Under the  $SU(3)$  flavor symmetry of  $u, d, s$  quarks, the light baryon octet  $T_8$ , the light baryon decuplet  $T_{10}$ , the light pseudoscalar meson octet  $P_8$ , and the vector meson octet  $V_8$  can be written as

$$T_8 = \begin{pmatrix} \frac{\Lambda^0}{\sqrt{6}} + \frac{\Sigma^0}{\sqrt{2}} & \Sigma^+ & p \\ \Sigma^- & \frac{\Lambda^0}{\sqrt{6}} - \frac{\Sigma^0}{\sqrt{2}} & n \\ \Xi^- & \Xi^0 & -\frac{2\Lambda^0}{\sqrt{6}} \end{pmatrix}, \quad (1)$$

$$T_{10} = \frac{1}{\sqrt{3}} \left( \begin{pmatrix} \sqrt{3}\Delta^{++} & \Delta^+ & \Sigma^{*+} \\ \Delta^+ & \Delta^0 & \frac{\Sigma^{*0}}{\sqrt{2}} \\ \Sigma^{*+} & \frac{\Sigma^{*0}}{\sqrt{2}} & \Xi^{*0} \end{pmatrix}, \begin{pmatrix} \Delta^+ & \Delta^0 & \frac{\Sigma^{*0}}{\sqrt{2}} \\ \Delta^0 & \sqrt{3}\Delta^- & \Sigma^{*-} \\ \frac{\Sigma^{*0}}{\sqrt{2}} & \Sigma^{*-} & \Xi^{*-} \end{pmatrix}, \begin{pmatrix} \Sigma^{*+} & \frac{\Sigma^{*0}}{\sqrt{2}} & \Xi^{*0} \\ \frac{\Sigma^{*0}}{\sqrt{2}} & \Sigma^{*-} & \Xi^{*-} \\ \Xi^{*-} & \Xi^{*-} & \sqrt{3}\Omega^- \end{pmatrix} \right), \quad (2)$$

$$P_8 = \begin{pmatrix} \frac{\eta_8}{\sqrt{6}} + \frac{\pi^0}{\sqrt{2}} & \pi^+ & K^+ \\ \pi^- & \frac{\eta_8}{\sqrt{6}} - \frac{\pi^0}{\sqrt{2}} & K^0 \\ K^- & \bar{K}^0 & -\sqrt{\frac{2}{3}}\eta_8 \end{pmatrix}, \quad (3)$$

$$V_8 = \begin{pmatrix} \frac{\omega_8}{\sqrt{6}} + \frac{\rho^0}{\sqrt{2}} & \rho^+ & K^{*+} \\ \rho^- & \frac{\omega_8}{\sqrt{6}} - \frac{\rho^0}{\sqrt{2}} & K^{*0} \\ K^{*-} & \bar{K}^{*0} & -\sqrt{\frac{2}{3}}\omega_8 \end{pmatrix}. \quad (4)$$

Two-body nonleptonic weak decays  $T_{8,10} \rightarrow T'_{8,10} M_8$  with  $M_8 = P_8, V_8$  are induced by  $s \rightarrow u\bar{u}d$  transition. As shown in Fig. 1, there are two kinds of diagrams for s-quark weak decay in the SM, the tree level diagram in Fig. 1 (a) and the penguin diagram in Fig. 1 (b). The effective Hamiltonian for nonleptonic  $s \rightarrow u\bar{u}d$  process at scales  $\mu < m_c$  can be written as [45]

$$\mathcal{H}_{eff} = \frac{G_F}{\sqrt{2}} V_{ud} V_{us}^* \sum_{i=1}^{10} \left[ z_i(\mu) - \frac{V_{td} V_{ts}^*}{V_{ud} V_{us}^*} y_i(\mu) \right] Q_i(\mu), \quad (5)$$

where  $V_{uq}$  is the CKM matrix element,  $z_i(\mu)$  and  $y_i(\mu)$  are Wilson coefficients, and  $Q_i$  is four-quark operators. We take  $V_{ud} V_{us}^* = \lambda(1 - \lambda^2/2) \approx 0.22$  and  $|V_{td} V_{ts}^*| = A^2 \lambda^5 |1 - \rho - i\eta| \approx 3.6 \times 10^{-4}$  from Ref. [1], and then redefine the Wilson coefficients  $C_i(\mu) \equiv z_i(\mu) - \frac{V_{td} V_{ts}^*}{V_{ud} V_{us}^*} y_i(\mu)$  at  $\mu = 1$  GeV on  $\Lambda_{\overline{MS}}^{(4)}$  in the NDR scheme are [45]

$$\begin{aligned} C_1 &= -0.625, & C_2 &= 1.361, & C_3 &= 0.023, & C_4 &= -0.058, & C_5 &= 0.009, & C_6 &= -0.059, \\ C_7/\alpha_e &= 0.021, & C_8/\alpha_e &= 0.027, & C_9/\alpha_e &= 0.036, & C_{10}/\alpha_e &= -0.015. \end{aligned} \quad (6)$$

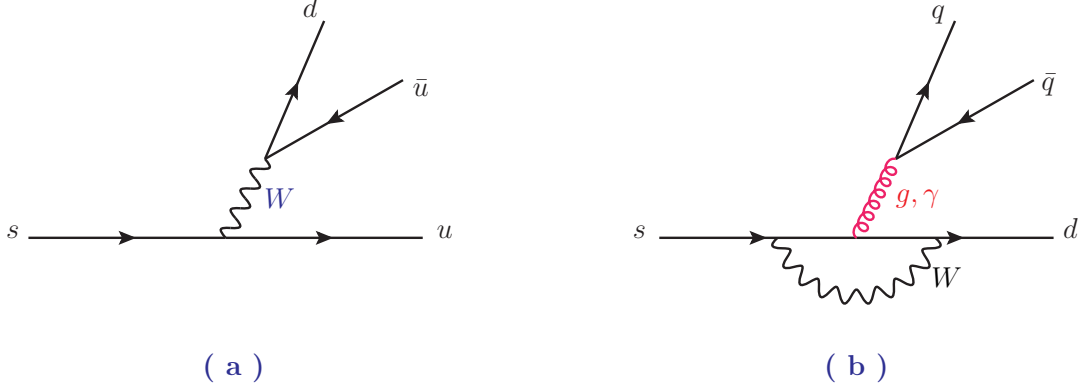


FIG. 1: Feynman diagrams for the  $s$  quark decays in the SM.

The four-quark operators  $Q_i$  are

$$\begin{aligned}
 Q_1 &= (\bar{d}_\alpha u_\beta)_{V-A} (\bar{u}_\beta s_\alpha)_{V-A}, & Q_2 &= (\bar{d}u)_{V-A} (\bar{u}s)_{V-A}, \\
 Q_{3,5} &= (\bar{d}s)_{V-A} \sum_{q=u,d,s} (\bar{q}q)_{V\mp A}, & Q_{4,6} &= (\bar{d}_\beta s_\alpha)_{V-A} \sum_{q=u,d,s} (\bar{q}_\alpha q_\beta)_{V\mp A}, \\
 Q_{7,9} &= \frac{3}{2} (\bar{d}s)_{V-A} \sum_{q=u,d,s} e_q (\bar{q}q)_{V\pm A}, & Q_{8,10} &= \frac{3}{2} (\bar{d}_\beta s_\alpha)_{V-A} \sum_{q=u,d,s} e_q (\bar{q}_\alpha q_\beta)_{V\pm A},
 \end{aligned} \tag{7}$$

where  $Q_{1,2}$  are current-current operators corresponding to Fig. 1 (a),  $Q_{3-6}$  ( $Q_{7-10}$ ) are QCD (electroweak) penguin operators corresponding to Fig. 1 (b).

The relevant topological diagrams for  $T_{8,10} \rightarrow T_8 M_8$  nonleptonic weak decays are displayed in Fig. 2. Since the octet baryon is not fully symmetric or antisymmetric in flavor space, there are more than one amplitudes corresponding to one topological diagram. Noted that Fig. 2 (c,  $\sigma$ ) only contributes the decays with  $M_8 = \eta, \omega$ , which will not be considered in this work. Other topological diagrams in Fig. 2 can be divided into three categories: the tree diagrams in Fig. 2 (a,b), the W-exchange diagrams in Fig. 2 (d,e,f,g) and the penguin diagrams in Fig. 2 ( $\lambda, \gamma$ ). Fig. 2 (a) contributes to the decays with the charged  $M_8$ , which is proportional to the color-flavor factor  $C_2 + \frac{C_1}{N_C}$ . Fig. 2 (b) contributes to the decays with the neutral  $M_8$ , which is proportional to  $C_1 + \frac{C_2}{N_C}$ . The contributions of Fig. 2 (d,e,f,g) are all proportional to  $C_2 - C_1$ . Compared with the tree diagrams and W-exchange contributions related to  $C_{1,2}$ , the penguin contributions displayed in Fig. 2 ( $\lambda, \gamma$ ) are strongly suppressed by small Wilson coefficients  $C_{3,\dots,10}$  and quite small CKM factor, and their contributions can be safely ignored in these decays if one do not consider the information of CP violation.

The branching ratios of the  $T_A \rightarrow T_B M_C$  two-body decays can be written in terms of the decay amplitudes  $A(T_A \rightarrow T_B M_C)$

$$\mathcal{B}(T_A \rightarrow T_B M_C) = \frac{\tau_A |p_{cm}|}{8\pi m_A^2} |A(T_A \rightarrow T_B M_C)|^2 S, \tag{8}$$

where  $|p_{cm}| = \sqrt{(m_A^2 - (m_B + m_C)^2)(m_A^2 - (m_B - m_C)^2)}/(2m_A)$ ,  $S = 1$  for  $T_A = T_8$ , and  $S = 1/2$  for  $T_A = T_{10}$ . For more accurate results, we will consider the mass difference in the amplitudes [46]

$$A(T_A \rightarrow T_B M_C) \propto \frac{m_A}{m_B} p_{cm} N_B N_A, \tag{9}$$

with  $N_A = \sqrt{2m_A}$  and  $N_B = \sqrt{((m_A + m_B)^2 - m_P^2)/(2m_A)}$ , and the amplitudes of  $A(T_A \rightarrow T_B M_C)$  for different decay processes are given in next section.

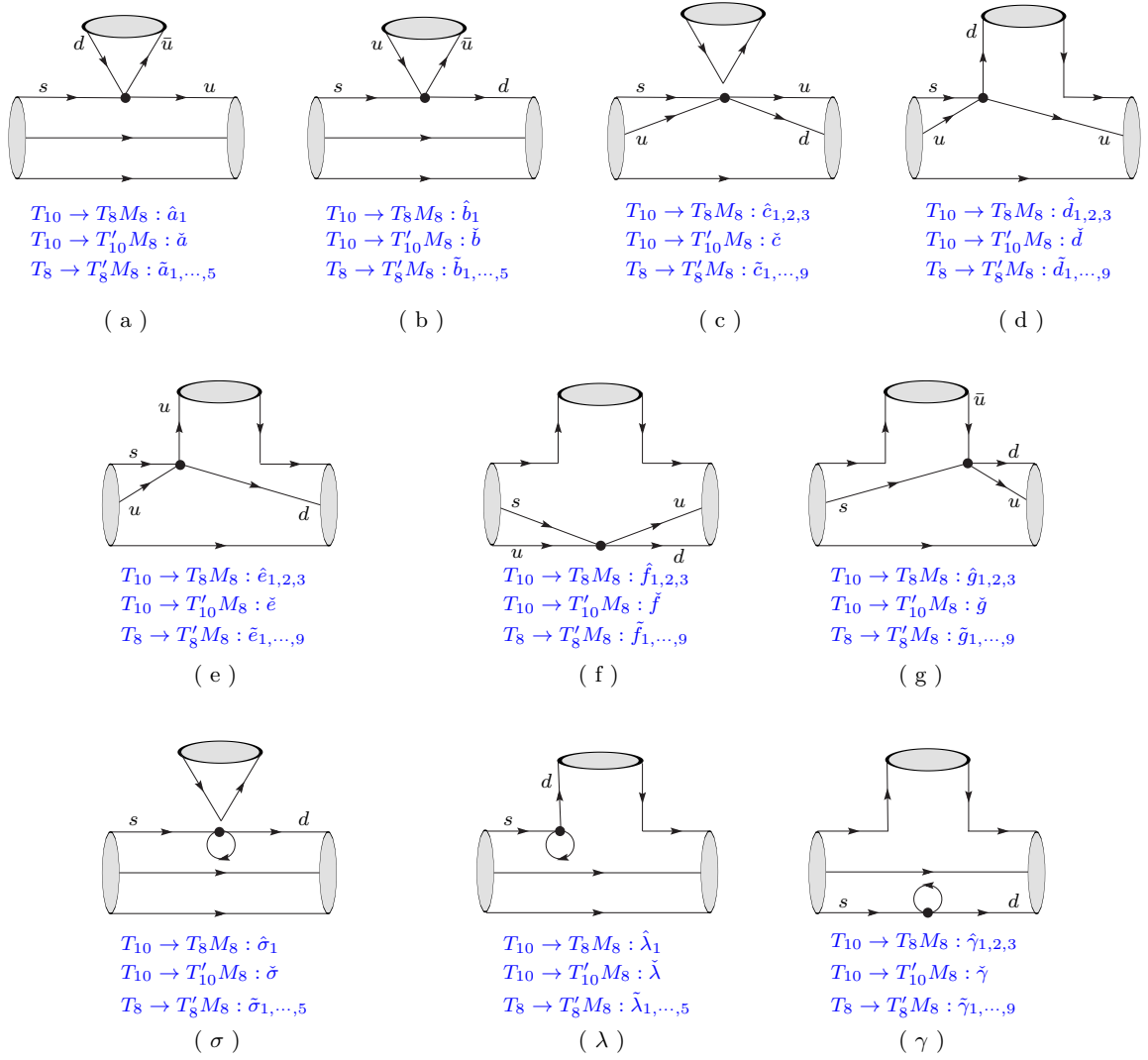


FIG. 2: Topological diagrams for  $T_{8,10} \rightarrow T'_{8,10} M_8$  nonleptonic decays. Since the octet baryon  $T_8$  is not fully asymmetric or antisymmetric in flavor space, there might be more than one amplitudes corresponding to one relevant topological diagram.

### III. Results and discussions

In this section, we only give the concrete amplitudes of  $T_{8,10} \rightarrow T'_{8,10} P_8$  decays, and the corresponding amplitudes of  $T_{8,10} \rightarrow T'_{8,10} V_8$  decays can be obtained similarly by replacing  $P_8$  to  $V_8$  in following Tab. I, Tab. III and Tab. V. For  $T_8 \rightarrow T_{10} M_8$  decays, the tree diagram contributions in Fig. 2 (a,b) and the penguin diagram contributions in Fig. 2 (σ, λ) are vanish, and according to Körner, Pati, Woo (KPW) theorem [47, 48], the W-exchange contribution is strongly suppressed since the contraction of the flavor antisymmetric current-current operator with a flavor symmetric final state configuration is zero, furthermore, we find that almost processes are not allowed by the phase spaces. So we will only give the detail analysis for  $T_{10} \rightarrow T_8 P_8$ ,  $T_{10} \rightarrow T'_{10} P_8$  and  $T_8 \rightarrow T'_8 P_8$  weak decays. In addition, the theoretical input parameters and the experimental data within the  $1\sigma$  error from Particle Data Group [1] will be used in our numerical results.

## A. $T_{10} \rightarrow T_8 M_8$ weak decays

Topological diagrams for  $T_{10} \rightarrow T_8 M_8$  decays are displayed in Fig. 2, and the TPA amplitudes of  $T_{10} \rightarrow T_8 M_8$  weak decays are

$$\begin{aligned}
A(T_{10} \rightarrow T_8 M_8)^{TPA} = & \hat{a}_1 H_{mn}'^{kl}(T_{10})^{nij}(T_8)_{[ik]j}(M_8)_l^m \\
& + \hat{b}_1 H_{mn}'^{kl}(T_{10})^{nij}(T_8)_{[il]j}(M_8)_k^m \\
& + \hat{c}_1 H_{kn}'^{il}(T_{10})^{nij}(T_8)_{[jk]l}(M_8)_m^m + \hat{c}_2 H_{kn}'^{il}(T_{10})^{nij}(T_8)_{[jl]k}(M_8)_m^m + \hat{c}_3 H_{kn}'^{il}(T_{10})^{nij}(T_8)_{[kl]j}(M_8)_m^m \\
& + \hat{d}_1 H_{in}'^{lk}(T_{10})^{nij}(T_8)_{[jm]k}(M_8)_l^m + \hat{d}_2 H_{in}'^{lk}(T_{10})^{nij}(T_8)_{[jk]m}(M_8)_l^m + \hat{d}_3 H_{in}'^{lk}(T_{10})^{nij}(T_8)_{[km]j}(M_8)_l^m \\
& + \hat{e}_1 H_{in}'^{kl}(T_{10})^{nij}(T_8)_{[jm]l}(M_8)_k^m + \hat{e}_2 H_{in}'^{kl}(T_{10})^{nij}(T_8)_{[jl]m}(M_8)_k^m + \hat{e}_3 H_{in}'^{kl}(T_{10})^{nij}(T_8)_{[lm]j}(M_8)_k^m \\
& + \hat{f}_1 H_{in}'^{kl}(T_{10})^{nij}(T_8)_{[kl]m}(M_8)_j^m + \hat{f}_2 H_{in}'^{kl}(T_{10})^{nij}(T_8)_{[km]l}(M_8)_j^m + \hat{f}_3 H_{in}'^{kl}(T_{10})^{nij}(T_8)_{[ml]k}(M_8)_j^m \\
& + \hat{g}_1 H_{mn}'^{lk}(T_{10})^{nij}(T_8)_{[ik]l}(M_8)_j^m + \hat{g}_2 H_{mn}'^{lk}(T_{10})^{nij}(T_8)_{[il]k}(M_8)_j^m + \hat{g}_3 H_{mn}'^{lk}(T_{10})^{nij}(T_8)_{[lk]i}(M_8)_j^m \\
& + \hat{\sigma}_1 H_{ln}'^{lk}(T_{10})^{nij}(T_8)_{[ik]j}(M_8)_m^m \\
& + \hat{\lambda}_1 H_{ln}'^{lk}(T_{10})^{nij}(T_8)_{[im]j}(M_8)_k^m \\
& + \hat{\gamma}_1 H_{ln}'^{lk}(T_{10})^{nij}(T_8)_{[ik]m}(M_8)_j^m + \hat{\gamma}_2 H_{ln}'^{lk}(T_{10})^{nij}(T_8)_{[im]k}(M_8)_j^m + \hat{\gamma}_3 H_{ln}'^{lk}(T_{10})^{nij}(T_8)_{[mk]i}(M_8)_j^m, (10)
\end{aligned}$$

where  $H_{mn}'^{kl} \equiv V_{mn} V_{kl}^*$  containing the CKM factors.

The TPA amplitudes for  $T_{10} \rightarrow T_8 P$  decays are given in Tab. I. Noted that  $\hat{f}_i$  terms in Fig. 2 (f) related to the  $T_{10} \rightarrow T_8 M_8$  decays only contribute to  $\Sigma^{*0} \rightarrow p\pi^-$ ,  $\Sigma^{*0} \rightarrow n\pi^0$  and  $\Sigma^{*+} \rightarrow p\pi^0$  processes, which are not allowed by the phase space. Comparing the SU(3) irreducible representation approach (IRA) amplitudes in Tab. VIII of Ref.

TABLE I: TPA amplitudes of  $T_{10} \rightarrow T_8 P$  decays under the  $s \rightarrow u\bar{d}$  transition. Noted that  $\hat{X}_1 \equiv \tilde{x}_1 - \tilde{x}_2 + 2\tilde{x}_3$  and  $\hat{X}_2 \equiv \tilde{x}_1 + \tilde{x}_2$  with  $\hat{X} = \hat{G}, \hat{\Gamma}, \hat{D}, \hat{E}$  for  $\hat{g}_i, \hat{\gamma}_i, \hat{d}_i, \hat{e}_i$ , respectively.

Observables	Tree	W-exchange	Penguin	Reparameterization
$A(\Omega^- \rightarrow \Xi^0 \pi^-)$	$\hat{a}_1$		$+\hat{\beta}_1$	$\hat{A}'_1$
$\sqrt{2}A(\Omega^- \rightarrow \Xi^- \pi^0)$	$-\hat{b}_1$		$+\hat{\beta}_1$	$\hat{A}'_2$
$\sqrt{6}A(\Omega^- \rightarrow \Lambda^0 K^-)$		$-\hat{G}_1$	$-\hat{\Gamma}_1$	$\hat{A}'_3$
$3\sqrt{2}A(\Xi^{*-} \rightarrow \Lambda^0 \pi^-)$	$3\hat{a}_1$	$-\hat{G}_1$	$+3\hat{\beta}_1 - \hat{\Gamma}_1$	$3\hat{A}'_1 + \hat{A}'_3$
$\sqrt{6}A(\Xi^{*-} \rightarrow \Sigma^0 \pi^-)$	$\hat{a}_1$	$+\hat{G}_2$	$+\hat{\beta}_1 + \hat{\Gamma}_2$	$\hat{A}'_1$
$\sqrt{6}A(\Xi^{*-} \rightarrow \Sigma^- \pi^0)$	$-\hat{b}_1$		$+\hat{\beta}_1 + \hat{\Gamma}_2$	$\hat{A}'_2$
$\sqrt{3}A(\Xi^{*0} \rightarrow \Sigma^+ \pi^-)$	$\hat{a}_1$	$+\hat{D}_2$	$+\hat{\beta}_1$	$\hat{A}'_1$
$\sqrt{3}A(\Xi^{*0} \rightarrow \Sigma^- \pi^+)$		$-\hat{E}_2$	$+\hat{\Gamma}_2$	$-\hat{E}_2$
$6A(\Xi^{*0} \rightarrow \Lambda^0 \pi^0)$	$-3\hat{b}_1$	$+\hat{D}_1 + \hat{E}_1 - \hat{G}_1$	$+3\hat{\beta}_1 - \hat{\Gamma}_1$	$3\hat{A}'_2 + \hat{A}'_3$
$2\sqrt{3}A(\Xi^{*0} \rightarrow \Sigma^0 \pi^0)$	$\hat{b}_1$	$-\hat{D}_2 + \hat{E}_2 + \hat{G}_2$	$-\hat{\beta}_1 + \hat{\Gamma}_2$	$-\hat{A}'_2$
$\sqrt{3}A(\Xi^{*-} \rightarrow nK^-)$		$(\hat{G}_1 - \hat{G}_2)/2$	$-(\hat{\Gamma}_2 - \hat{\Gamma}_1)/2$	$-\hat{A}'_3/2$
$\sqrt{3}A(\Sigma^{*-} \rightarrow n\pi^-)$	$-\hat{a}_1$	$+(\hat{G}_1 - \hat{G}_2)/2$	$-\hat{\beta}_1 - (\hat{\Gamma}_2 - \hat{\Gamma}_1)/2$	$-\hat{A}'_1 - \hat{A}'_3/2$

[28] with the TPA amplitudes in Tab. I, we have the following relations

$$\begin{aligned}
\bar{a}_1 &= \frac{\hat{a}_1 + \hat{b}_1}{4}, & \bar{e}_1 &= \frac{\hat{a}_1 - \hat{b}_1 + 2\hat{\beta}_1}{4}, & \bar{b}_2 &= -\frac{\hat{G}_2}{4}, \\
\bar{c}_3 + \bar{c}_2 &= \hat{D}_2 = \hat{E}_2, & 2\bar{c}_1 + \bar{c}_2 + \bar{c}_3 &= \frac{\hat{D}_1 + \hat{E}_1}{2}, \\
\bar{f}_1 + \bar{f}_2 &= \frac{\hat{G}_1 + \hat{\Gamma}_1}{2}, & \bar{f}_1 &= \bar{f}_3, & \hat{\Gamma}_2 &= 0.
\end{aligned} \tag{11}$$

From Eq. (11) one can see that the parameters  $\hat{G}_2, \hat{D}_1 + \hat{E}_1, \hat{D}_2$  and  $\hat{E}_2$  terms in TPA amplitudes are related to  $\bar{b}_2$  or  $\bar{c}_{1,2,3}$  terms in IRA amplitudes, which only appear in the Wilson coefficient suppressed  $C_+$  term, so we will neglect their contributions in following numerical analysis. Finally, the TPA amplitudes of relevant  $T_{10} \rightarrow T_8 P$  decays can be reparameterized by

$$\begin{aligned}
\hat{A}'_1 &\equiv \hat{a}_1 + \hat{\beta}_1, \\
\hat{A}'_2 &\equiv -\hat{b}_1 + \hat{\beta}_1, \\
\hat{A}'_3 &\equiv -(\hat{G}_1 + \hat{\Gamma}_1).
\end{aligned} \tag{12}$$

And the reparameterization TPA amplitudes are listed in the last column of Tab. I. Using the amplitude relations listed in the last column of Tab. I and the experimental data of  $\mathcal{B}(\Omega \rightarrow \Xi^0 \pi^-, \Xi^- \pi^0, \Lambda^0 K^-)$ , we obtain the predictions of the branching ratios for relevant  $\Xi^{*-}, \Xi^{*0}$  and  $\Sigma^{*-}$  decays, which are listed in the last column of Tab. II. Noted that the mass difference in the amplitudes similar to Eq. (9) is also considered. One can see that all branching ratios of  $\Xi^{*-}, \Xi^{*0}$  and  $\Sigma^{*-}$  decays are in the range of  $10^{-14} - 10^{-12}$  since their lifetimes are very small.

TABLE II: Branching ratios of  $T_{10} \rightarrow T_8 P_8$  decays within  $1\sigma$  error under the  $s \rightarrow u\bar{u}d$  transition. <sup>†</sup> denotes that the predictions depend on the relative phases.

Branching ratios	Exp. [1]	IRA [28]	TPA
$\mathcal{B}(\Omega^- \rightarrow \Xi^0 \pi^-)(\times 10^{-2})$	$23.6 \pm 0.7$	$23.6 \pm 0.7^\ddagger$	$23.6 \pm 0.7$
$\mathcal{B}(\Omega^- \rightarrow \Xi^- \pi^0)(\times 10^{-2})$	$8.6 \pm 0.4$	$8.6 \pm 0.4^\ddagger$	$8.6 \pm 0.4$
$\mathcal{B}(\Omega^- \rightarrow \Lambda^0 K^-)(\times 10^{-2})$	$67.8 \pm 0.7$	$67.8 \pm 0.7^\ddagger$	$67.8 \pm 0.7$
$\mathcal{B}(\Xi^{*-} \rightarrow \Lambda^0 \pi^-)(\times 10^{-12})$	...	$1.06 \pm 0.90^\dagger$	$1.06 \pm 0.90^\dagger$
$\mathcal{B}(\Xi^{*-} \rightarrow \Sigma^0 \pi^-)(\times 10^{-14})$	...	...	$2.87 \pm 0.65$
$\mathcal{B}(\Xi^{*-} \rightarrow \Sigma^- \pi^0)(\times 10^{-14})$	...	...	$2.14 \pm 0.52$
$\mathcal{B}(\Xi^{*0} \rightarrow \Sigma^+ \pi^-)(\times 10^{-14})$	...	$5.96 \pm 0.58$	$5.96 \pm 0.58$
$\mathcal{B}(\Xi^{*0} \rightarrow \Lambda^0 \pi^0)(\times 10^{-13})$	...	$5.02 \pm 4.06^\dagger$	$5.02 \pm 4.06^\dagger$
$\mathcal{B}(\Xi^{*0} \rightarrow \Sigma^0 \pi^0)(\times 10^{-14})$	...	...	$1.12 \pm 0.13$
$\mathcal{B}(\Xi^{*-} \rightarrow n K^-)(\times 10^{-13})$	...	...	$6.14 \pm 1.31$
$\mathcal{B}(\Sigma^{*-} \rightarrow n \pi^-)(\times 10^{-13})$	...	...	$3.84 \pm 2.41^\dagger$

## B. $T_{10} \rightarrow T'_{10} M_8$ weak decays

For  $T_{10} \rightarrow T'_{10} M_8$  decays, their amplitudes are simple since both initial state  $T_{10}$  and final state  $T'_{10}$  are all fully symmetric in flavor space. The TPA amplitudes of  $T_{10} \rightarrow T'_{10} M_8$  decays are

$$\begin{aligned}
A(T_{10} \rightarrow T'_{10} M_8)^{TPA} = & \check{a} H'_{mn}{}^{kl}(T_{10})^{nij}(T_{10})_{ijk}(M_8)_l^m + \check{b} H'_{mn}{}^{kl}(T_{10})^{nij}(T_{10})_{ijl}(M_8)_k^m \\
& + \check{c} H'_{in}{}^{kl}(T_{10})^{nij}(T_{10})_{klj}(M_8)_m^m + \check{d} H'_{in}{}^{kl}(T_{10})^{nij}(T_{10})_{mkj}(M_8)_l^m \\
& + \check{e} H'_{in}{}^{kl}(T_{10})^{nij}(T_{10})_{mlj}(M_8)_k^m + \check{f} H'_{in}{}^{kl}(T_{10})^{nij}(T_{10})_{lkm}(M_8)_j^m \\
& + \check{g} H'_{mn}{}^{lk}(T_{10})^{nij}(T_{10})_{ilk}(M_8)_j^m + \check{\sigma} H'_{ln}{}^{lk}(T_{10})^{nij}(T_{10})_{kij}(M_8)_m^m \\
& + \check{\lambda} H'_{ln}{}^{lk}(T_{10})^{nij}(T_{10})_{mij}(M_8)_k^m + \check{\gamma} H'_{ln}{}^{lk}(T_{10})^{nij}(T_{10})_{ikm}(M_8)_j^m.
\end{aligned} \tag{13}$$

And the TPA amplitudes for  $T_{10} \rightarrow T'_{10} P_8$  decays are given in Tab. III. Since the SU(3) IRA amplitudes of  $T_{10} \rightarrow T'_{10} M_8$  decays have not been calculated in Ref. [28], we give them in this paper. The IRA amplitudes of  $T_{10} \rightarrow T'_{10} M_8$  decays are

$$\begin{aligned}
A(T_{10} \rightarrow T'_{10} M_8)^{IRA} = & \ddot{a} H(4)_m^{lk}(T_{10})^{ijn}(T_{10})_{ijk}(M_8)_l^m + \ddot{b} H(4)_m^{lk}(T_{10})^{ijn}(T_{10})_{ilk}(M_8)_j^m \\
& + \ddot{c} H(4)_j^{lk}(T_{10})^{ijn}(T_{10})_{imk}(M_8)_l^m + \ddot{d} H(4)_j^{lk}(T_{10})^{ijn}(T_{10})_{mlk}(M_8)_i^m \\
& + \ddot{e} H(\bar{2})^k(T_{10})^{ijn}(T_{10})_{ijm}(M_8)_k^m + \ddot{f} H(\bar{2})^k(T_{10})^{ijn}(T_{10})_{kim}(M_8)_j^m.
\end{aligned} \tag{14}$$

And the concrete amplitudes for  $T_{10} \rightarrow T'_{10} P_8$  decays are given in Tab. IV. We find that the TPA and the IRA match consistently in  $T_{10} \rightarrow T'_{10} M_8$  decays, and the relations between the two sets of amplitudes are

$$\begin{aligned}
\ddot{a} + \ddot{e} &= \check{a} + \check{\beta}, & 2\ddot{a} - \ddot{a}' &= \check{a} + \check{b}, & 2\ddot{b} + \ddot{f} &= \check{g}, \\
\ddot{c} &= \check{d} = \check{e}, & \ddot{d} &= \frac{1}{2}\check{f}, \\
\ddot{f} &= -\check{b}', & \check{\gamma} &= 0.
\end{aligned} \tag{15}$$

From the Tab. III, we have the following amplitude relations

$$\begin{aligned}
A(\Omega^- \rightarrow \Xi^{*-} \pi^0) &= \sqrt{3} A(\Xi^{*-} \rightarrow \Sigma^{*-} \pi^0), \\
\sqrt{2} A(\Omega^- \rightarrow \Sigma^{*0} K^-) &= \sqrt{3} A(\Xi^{*-} \rightarrow \Delta^0 K^-), \\
\sqrt{6} A(\Xi^{*-} \rightarrow \Sigma^{*0} \pi^-) &= A(\Omega^- \rightarrow \Xi^{*0} \pi^-) + \sqrt{2} A(\Omega^- \rightarrow \Sigma^{*0} K^-) \\
&= A(\Omega^- \rightarrow \Xi^{*0} \pi^-) + \sqrt{2} A(\Xi^{*-} \rightarrow \Delta^0 K^-).
\end{aligned} \tag{16}$$

In Refs. [47, 48], the W-exchange contribution in  $T_{10} \rightarrow T'_{10} M_8$  decays is strongly suppressed since the contraction of the flavor antisymmetric current-current operator with a flavor symmetric final state configuration is zero. So we can safely ignore the W-exchange diagrams and the small penguin diagram contributions in  $T_{10} \rightarrow T'_{10} M_8$  decays, and then we have very simple relations

$$\begin{aligned}
A(\Omega^- \rightarrow \Xi^{*-} \pi^0) &= \sqrt{6} A(\Xi^{*0} \rightarrow \Sigma^{*0} \pi^0) = \sqrt{3} A(\Xi^{*-} \rightarrow \Sigma^{*-} \pi^0), \\
A(\Omega^- \rightarrow \Xi^{*0} \pi^-) &= \sqrt{3} A(\Xi^{*0} \rightarrow \Sigma^{*+} \pi^-) = \sqrt{6} A(\Xi^{*-} \rightarrow \Sigma^{*0} \pi^-).
\end{aligned} \tag{17}$$

From Eq. (17), in terms of the central values of the input parameters, one may get the ratios of their branching ratios

$$\begin{aligned}
\mathcal{B}(\Omega^- \rightarrow \Xi^{*0} \pi^-) : \mathcal{B}(\Xi^{*0} \rightarrow \Sigma^{*+} \pi^-) : \mathcal{B}(\Xi^{*-} \rightarrow \Sigma^{*0} \pi^-) &\approx 1 : 7.9 \times 10^{-12} : 5.1 \times 10^{-12}, \\
\mathcal{B}(\Omega^- \rightarrow \Xi^{*-} \pi^0) : \mathcal{B}(\Xi^{*0} \rightarrow \Sigma^{*0} \pi^0) : \mathcal{B}(\Xi^{*-} \rightarrow \Sigma^{*-} \pi^0) &\approx 1 : 1.9 \times 10^{-12} : 3.3 \times 10^{-12}.
\end{aligned} \tag{18}$$

TABLE III: TPA amplitudes of  $T_{10} \rightarrow T'_{10} P_8$  decays under the  $s \rightarrow u\bar{u}d$  transition.

Observables	Tree	W-exchange	Penguin
$\sqrt{6}A(\Omega^- \rightarrow \Xi^{*-}\pi^0)$	$\check{b}$		$-\check{\beta}$
$\sqrt{3}A(\Omega^- \rightarrow \Xi^{*0}\pi^-)$	$\check{a}$		$+\check{\beta}$
$\sqrt{6}A(\Omega^- \rightarrow \Sigma^{*0}K^-)$		$\check{g}$	$+\check{\gamma}$
$6A(\Xi^{*0} \rightarrow \Sigma^{*0}\pi^0)$	$\check{b}$	$-\check{d} + \check{e} + \check{g}$	$-\check{\beta} + \check{\gamma}$
$3A(\Xi^{*0} \rightarrow \Sigma^{*+}\pi^-)$	$\check{a}$	$+\check{d}$	$+\check{\beta}$
$3A(\Xi^{*0} \rightarrow \Delta^+K^-)$		$\check{f} + \check{g}$	$+\check{\gamma}$
$3A(\Xi^{*0} \rightarrow \Sigma^{*-}\pi^+)$		$\check{e}$	$+\check{\gamma}$
$3A(\Xi^{*0} \rightarrow \Delta^0K^0)$		$\check{f}$	$\check{\gamma}$
$3\sqrt{2}A(\Xi^{*-} \rightarrow \Sigma^{*-}\pi^0)$	$\check{b}$		$-\check{\beta}$
$3\sqrt{2}A(\Xi^{*-} \rightarrow \Sigma^{*0}\pi^-)$	$\check{a}$	$+\check{g}$	$+\check{\beta} + \check{\gamma}$
$3A(\Xi^{*-} \rightarrow \Delta^0K^-)$		$\check{g}$	$+\check{\gamma}$

TABLE IV: The SU(3) IRA amplitudes of  $T_{10} \rightarrow T'_{10} P_8$  decays under the  $s \rightarrow u\bar{u}d$  transition. Noted that  $\check{a}'$  and  $\check{b}'$  denote  $\check{a}$  and  $\check{b}$  terms in  $H(4)_2^{22}$ , respectively.

Observables	$H(4)_1^{12} = \frac{1}{3}$	$H(4)_2^{22} = -\frac{1}{3}$	$H(\bar{2})^2 = 1$
$\sqrt{6}A(\Omega^- \rightarrow \Xi^{*-}\pi^0)$	$\check{a}$	$-\check{a}'$	$-\check{e}$
$\sqrt{3}A(\Omega^- \rightarrow \Xi^{*0}\pi^-)$	$\check{a}$		$+\check{e}$
$\sqrt{6}A(\Omega^- \rightarrow \Sigma^{*0}K^-)$	$2\check{b}$		$+\check{f}$
$6A(\Xi^{*0} \rightarrow \Sigma^{*0}\pi^0)$	$\check{a} + 2\check{b}$	$-\check{a}'$	$-\check{e} + \check{f}$
$3A(\Xi^{*0} \rightarrow \Sigma^{*+}\pi^-)$	$\check{a} + \check{c}$		$+\check{e}$
$3A(\Xi^{*0} \rightarrow \Delta^+K^-)$	$2\check{b} + 2\check{d}$		$+\check{f}$
$3A(\Xi^{*0} \rightarrow \Sigma^{*-}\pi^+)$	$\check{c}$	$+\check{b}'$	$+\check{f}$
$3A(\Xi^{*0} \rightarrow \Delta^0K^0)$	$2\check{d}$	$+\check{b}'$	$\check{f}$
$3\sqrt{2}A(\Xi^{*-} \rightarrow \Sigma^{*-}\pi^0)$	$\check{a}$	$-\check{a}' - \check{b}'$	$-\check{e} - \check{f}$
$3\sqrt{2}A(\Xi^{*-} \rightarrow \Sigma^{*0}\pi^-)$	$\check{a} + 2\check{b}$		$+\check{e} + \check{f}$
$3A(\Xi^{*-} \rightarrow \Delta^0K^-)$	$2\check{b}$		$+\check{f}$



From the experimental upper limit  $\mathcal{B}(\Omega^- \rightarrow \Xi^{*0}\pi^-) < 7 \times 10^{-5}$  at 90% CL [1], considering the  $1\sigma$  error of relevant input parameters, we obtain that

$$\begin{aligned}\mathcal{B}(\Xi^{*0} \rightarrow \Sigma^{*+}\pi^-) &< 2.1 \times 10^{-15}, \\ \mathcal{B}(\Xi^{*-} \rightarrow \Sigma^{*0}\pi^-) &< 1.5 \times 10^{-15}.\end{aligned}\tag{19}$$

### C. $T_8 \rightarrow T'_8 M_8$ weak decays

Topological diagrams for  $T_8 \rightarrow T'_8 M_8$  are displayed in Fig. 2. Since both initial state  $T_8$  and final state  $T'_8$  are all not fully symmetric or antisymmetric in flavor space, there are many amplitudes corresponding to one topological diagram, as a result, 92 amplitudes for  $T_8 \rightarrow T'_8 M_8$  decays correspond to 10 topological diagrams in Fig. 2. The TPA amplitudes of  $T_8 \rightarrow T'_8 M_8$  decays can be constructed as

$$\begin{aligned}A(T_8 \rightarrow T'_8 M_8)^{TPA} = & \tilde{a}_1 H_{mn}^{kl}(T_8)^{[ij]n}(T_8)_{[ij]k}(M_8)_l^m + \tilde{a}_2 H_{mn}^{kl}(T_8)^{[ij]n}(T_8)_{[ik]j}(M_8)_l^m \\ & + \tilde{a}_3 H_{mn}^{kl}(T_8)^{[in]j}(T_8)_{[ij]k}(M_8)_l^m + \tilde{a}_4 H_{mn}^{kl}(T_8)^{[in]j}(T_8)_{[ik]j}(M_8)_l^m + \tilde{a}_5 H_{mn}^{kl}(T_8)^{[in]j}(T_8)_{[kj]i}(M_8)_l^m \\ & + \tilde{b}_1 H_{mn}^{kl}(T_8)^{[ij]n}(T_8)_{[ij]l}(M_8)_k^m + \tilde{b}_2 H_{mn}^{kl}(T_8)^{[ij]n}(T_8)_{[il]j}(M_8)_k^m \\ & + \tilde{b}_3 H_{mn}^{kl}(T_8)^{[in]j}(T_8)_{[ij]l}(M_8)_k^m + \tilde{b}_4 H_{mn}^{kl}(T_8)^{[in]j}(T_8)_{[il]j}(M_8)_k^m + \tilde{b}_5 H_{mn}^{kl}(T_8)^{[in]j}(T_8)_{[lj]i}(M_8)_k^m \\ & + \tilde{c}_1 H_{in}^{lk}(T_8)^{[ij]n}(T_8)_{[jk]l}(M_8)_m^m + \tilde{c}_2 H_{in}^{lk}(T_8)^{[ij]n}(T_8)_{[jl]k}(M_8)_m^m + \tilde{c}_3 H_{in}^{lk}(T_8)^{[ij]n}(T_8)_{[kl]j}(M_8)_m^m \\ & + \tilde{c}_4 H_{in}^{lk}(T_8)^{[in]j}(T_8)_{[jk]l}(M_8)_m^m + \tilde{c}_5 H_{in}^{lk}(T_8)^{[in]j}(T_8)_{[jl]k}(M_8)_m^m + \tilde{c}_6 H_{in}^{lk}(T_8)^{[in]j}(T_8)_{[kl]j}(M_8)_m^m \\ & + \tilde{c}_7 H_{in}^{lk}(T_8)^{[jn]i}(T_8)_{[jk]l}(M_8)_m^m + \tilde{c}_8 H_{in}^{lk}(T_8)^{[jn]i}(T_8)_{[jl]k}(M_8)_m^m + \tilde{c}_9 H_{in}^{lk}(T_8)^{[jn]i}(T_8)_{[kl]j}(M_8)_m^m \\ & + \tilde{d}_1 H_{in}^{lk}(T_8)^{[ij]n}(T_8)_{[jm]k}(M_8)_l^m + \tilde{d}_2 H_{in}^{lk}(T_8)^{[ij]n}(T_8)_{[jk]m}(M_8)_l^m + \tilde{d}_3 H_{in}^{lk}(T_8)^{[ij]n}(T_8)_{[km]j}(M_8)_l^m \\ & + \tilde{d}_4 H_{in}^{lk}(T_8)^{[in]j}(T_8)_{[jm]k}(M_8)_l^m + \tilde{d}_5 H_{in}^{lk}(T_8)^{[in]j}(T_8)_{[jk]m}(M_8)_l^m + \tilde{d}_6 H_{in}^{lk}(T_8)^{[in]j}(T_8)_{[km]j}(M_8)_l^m \\ & + \tilde{d}_7 H_{in}^{lk}(T_8)^{[jn]i}(T_8)_{[jm]k}(M_8)_l^m + \tilde{d}_8 H_{in}^{lk}(T_8)^{[jn]i}(T_8)_{[jk]m}(M_8)_l^m + \tilde{d}_9 H_{in}^{lk}(T_8)^{[jn]i}(T_8)_{[km]j}(M_8)_l^m \\ & + \tilde{e}_1 H_{in}^{lk}(T_8)^{[ij]n}(T_8)_{[jm]l}(M_8)_k^m + \tilde{e}_2 H_{in}^{lk}(T_8)^{[ij]n}(T_8)_{[jl]m}(M_8)_k^m + \tilde{e}_3 H_{in}^{lk}(T_8)^{[ij]n}(T_8)_{[lm]j}(M_8)_k^m \\ & + \tilde{e}_4 H_{in}^{lk}(T_8)^{[in]j}(T_8)_{[jm]l}(M_8)_k^m + \tilde{e}_5 H_{in}^{lk}(T_8)^{[in]j}(T_8)_{[jl]m}(M_8)_k^m + \tilde{e}_6 H_{in}^{lk}(T_8)^{[in]j}(T_8)_{[lm]j}(M_8)_k^m \\ & + \tilde{e}_7 H_{in}^{lk}(T_8)^{[jn]i}(T_8)_{[jm]l}(M_8)_k^m + \tilde{e}_8 H_{in}^{lk}(T_8)^{[jn]i}(T_8)_{[jl]m}(M_8)_k^m + \tilde{e}_9 H_{in}^{lk}(T_8)^{[jn]i}(T_8)_{[lm]j}(M_8)_k^m \\ & + \tilde{f}_1 H_{in}^{lk}(T_8)^{[ij]n}(T_8)_{[kl]m}(M_8)_j^m + \tilde{f}_2 H_{in}^{lk}(T_8)^{[ij]n}(T_8)_{[km]l}(M_8)_j^m + \tilde{f}_3 H_{in}^{lk}(T_8)^{[ij]n}(T_8)_{[ml]k}(M_8)_j^m \\ & + \tilde{f}_4 H_{in}^{lk}(T_8)^{[in]j}(T_8)_{[kl]m}(M_8)_j^m + \tilde{f}_5 H_{in}^{lk}(T_8)^{[in]j}(T_8)_{[km]l}(M_8)_j^m + \tilde{f}_6 H_{in}^{lk}(T_8)^{[in]j}(T_8)_{[ml]k}(M_8)_j^m \\ & + \tilde{f}_7 H_{in}^{lk}(T_8)^{[jn]i}(T_8)_{[kl]m}(M_8)_j^m + \tilde{f}_8 H_{in}^{lk}(T_8)^{[jn]i}(T_8)_{[km]l}(M_8)_j^m + \tilde{f}_9 H_{in}^{lk}(T_8)^{[jn]i}(T_8)_{[ml]k}(M_8)_j^m \\ & + \tilde{g}_1 H_{mn}^{lk}(T_8)^{[ij]n}(T_8)_{[ik]l}(M_8)_j^m + \tilde{g}_2 H_{mn}^{lk}(T_8)^{[ij]n}(T_8)_{[il]k}(M_8)_j^m + \tilde{g}_3 H_{mn}^{lk}(T_8)^{[ij]n}(T_8)_{[lk]i}(M_8)_j^m \\ & + \tilde{g}_4 H_{mn}^{lk}(T_8)^{[in]j}(T_8)_{[ik]l}(M_8)_j^m + \tilde{g}_5 H_{mn}^{lk}(T_8)^{[in]j}(T_8)_{[il]k}(M_8)_j^m + \tilde{g}_6 H_{mn}^{lk}(T_8)^{[in]j}(T_8)_{[lk]i}(M_8)_j^m \\ & + \tilde{g}_7 H_{mn}^{lk}(T_8)^{[jn]i}(T_8)_{[ik]l}(M_8)_j^m + \tilde{g}_8 H_{mn}^{lk}(T_8)^{[jn]i}(T_8)_{[il]k}(M_8)_j^m + \tilde{g}_9 H_{mn}^{lk}(T_8)^{[jn]i}(T_8)_{[lk]i}(M_8)_j^m \\ & + \tilde{\sigma}_1 H_{ln}^{lk}(T_8)^{[ij]n}(T_8)_{[ij]k}(M_8)_m^m + \tilde{\sigma}_2 H_{ln}^{lk}(T_8)^{[ij]n}(T_8)_{[ik]j}(M_8)_m^m \\ & + \tilde{\sigma}_3 H_{ln}^{lk}(T_8)^{[in]j}(T_8)_{[ij]k}(M_8)_m^m + \tilde{\sigma}_4 H_{ln}^{lk}(T_8)^{[in]j}(T_8)_{[ik]j}(M_8)_m^m + \tilde{\sigma}_5 H_{ln}^{lk}(T_8)^{[in]j}(T_8)_{[kj]i}(M_8)_m^m \\ & + \tilde{\lambda}_1 H_{ln}^{lk}(T_8)^{[ij]n}(T_8)_{[ij]m}(M_8)_k^m + \tilde{\lambda}_2 H_{ln}^{lk}(T_8)^{[ij]n}(T_8)_{[im]j}(M_8)_k^m \\ & + \tilde{\lambda}_3 H_{ln}^{lk}(T_8)^{[in]j}(T_8)_{[ij]m}(M_8)_k^m + \tilde{\lambda}_4 H_{ln}^{lk}(T_8)^{[in]j}(T_8)_{[im]j}(M_8)_k^m + \tilde{\lambda}_5 H_{ln}^{lk}(T_8)^{[in]j}(T_8)_{[mj]i}(M_8)_k^m \\ & + \tilde{\gamma}_1 H_{ln}^{lk}(T_8)^{[ij]n}(T_8)_{[ik]m}(M_8)_j^m + \tilde{\gamma}_2 H_{ln}^{lk}(T_8)^{[ij]n}(T_8)_{[im]k}(M_8)_j^m + \tilde{\gamma}_3 H_{ln}^{lk}(T_8)^{[ij]n}(T_8)_{[mk]i}(M_8)_j^m \\ & + \tilde{\gamma}_4 H_{ln}^{lk}(T_8)^{[in]j}(T_8)_{[ik]m}(M_8)_j^m + \tilde{\gamma}_5 H_{ln}^{lk}(T_8)^{[in]j}(T_8)_{[im]k}(M_8)_j^m + \tilde{\gamma}_6 H_{ln}^{lk}(T_8)^{[in]j}(T_8)_{[mk]i}(M_8)_j^m \\ & + \tilde{\gamma}_7 H_{ln}^{lk}(T_8)^{[jn]i}(T_8)_{[ik]m}(M_8)_j^m + \tilde{\gamma}_8 H_{ln}^{lk}(T_8)^{[jn]i}(T_8)_{[im]k}(M_8)_j^m + \tilde{\gamma}_9 H_{ln}^{lk}(T_8)^{[jn]i}(T_8)_{[mk]i}(M_8)_j^m.\end{aligned}\tag{20}$$

From Eq. (20), we can get the TPA amplitudes of different decay modes. Since many parameters are not independent, we give the redefinitions

$$\begin{aligned} X_1 &\equiv 2\tilde{x}_1 + 2\tilde{x}_2 + 2\tilde{x}_3 + \tilde{x}_4 + \tilde{x}_5, \\ X_2 &\equiv \tilde{x}_4 - \tilde{x}_5, \end{aligned} \quad (21)$$

where  $X = A, B, \Sigma, \Lambda$  corresponding to  $\tilde{a}_i, \tilde{b}_i, \tilde{\sigma}_i, \tilde{\lambda}_i$ , respectively, and

$$\begin{aligned} Y_1 &\equiv \tilde{y}_1 + \tilde{y}_3 + \tilde{y}_4 + \tilde{y}_6, \\ Y_2 &\equiv \tilde{y}_4 + \tilde{y}_6 + \tilde{y}_7 + \tilde{y}_9, \\ Y_3 &\equiv \tilde{y}_4 + \tilde{y}_5 + \tilde{y}_7 + \tilde{y}_8, \\ Y_4 &\equiv \tilde{y}_2 - \tilde{y}_3 + \tilde{y}_5 - \tilde{y}_6, \end{aligned} \quad (22)$$

with  $Y = C, D, E, F, G, \Gamma$  for  $\tilde{c}_i, \tilde{d}_i, \tilde{e}_i, \tilde{f}_i, \tilde{g}_i, \tilde{\gamma}_i$ , respectively. And then the parameters related to  $T_8 \rightarrow T'_8 M_8$  decays studied in this paper are reduced to 26. The corresponding amplitudes are listed in Tab. V. Even if neglecting 6 small penguin amplitudes, there still are 20 parameters. Since the parameters are too much, it's difficult for us to find many relations between different decay amplitudes. And there is only one relation for the decay amplitudes

$$\sqrt{2}A(\Sigma^+ \rightarrow p\pi^0) = A(\Sigma^+ \rightarrow n\pi^+) + A(\Sigma^- \rightarrow n\pi^-) + \sqrt{2}A(\Sigma^0 \rightarrow p\pi^-) + 2A(\Sigma^0 \rightarrow n\pi^0), \quad (23)$$

in which includes the tree diagram, W-exchange diagram and the penguin diagram amplitudes.

Many  $T_8 \rightarrow T'_8 P_8$  decays have been measured [1]

$$\begin{aligned} \mathcal{B}(\Sigma^+ \rightarrow p\pi^0) &= (51.57 \pm 0.30) \times 10^{-2}, \\ \mathcal{B}(\Sigma^+ \rightarrow n\pi^+) &= (48.31 \pm 0.30) \times 10^{-2}, \\ \mathcal{B}(\Sigma^- \rightarrow n\pi^-) &= (99.848 \pm 0.005) \times 10^{-2}, \end{aligned}$$

TABLE V: TPA amplitudes of  $T_8 \rightarrow T'_8 P_8$  decays under the  $s \rightarrow u\bar{u}d$  transition.

Amplitudes	Tree	W-exchange	Penguin	Ratios of amplitude moduli
$\sqrt{2}A(\Sigma^+ \rightarrow p\pi^0)$	$-B_2$	$+D_2 + E_2 - E_3 - F_2 - G_2$	$+2\Lambda_2 - \Gamma_2$	2.02
$A(\Sigma^+ \rightarrow n\pi^+)$		$-E_3 - F_1$	$-\Gamma_3$	1.01
$A(\Sigma^- \rightarrow n\pi^-)$	$-A_2$	$+G_2 - G_3$	$-2\Lambda_2 + \Gamma_2 - \Gamma_3$	1.00
$\sqrt{2}A(\Sigma^0 \rightarrow p\pi^-)$	$A_2$	$+D_3 - F_2 - G_2$	$+2\Lambda_2 - \Gamma_2$	2.02
$2A(\Sigma^0 \rightarrow n\pi^0)$	$-B_2$	$+D_2 - D_3 + E_2 + F_1 - G_2 + G_3$	$+2\Lambda_2 - \Gamma_2 + 2\Gamma_3$	2.83
$\sqrt{6}A(\Lambda^0 \rightarrow p\pi^-)$	$-A_1$	$\frac{+2D_1 - D_3 + 2D_4}{-2F_1 + F_2 - 2G_1 + G_2}$	$-2\Lambda_1 - 2\Gamma_1 + \Gamma_2$	9.95
$2\sqrt{3}A(\Lambda^0 \rightarrow n\pi^0)$	$-B_1$	$\frac{-D_2 + D_3 - 2D_4 + 2E_1 - E_2}{+2F_1 - F_3 + 2F_4 - G_2 + G_3 - 2G_4}$	$+2\Lambda_1 + 2\Gamma_1 - \Gamma_2$	14.17
$\sqrt{6}A(\Xi^- \rightarrow \Lambda^0 \pi^-)$	$\frac{1}{2}A_1 + \frac{3}{2}A_2$	$+G_1 - 2G_2 + G_3 - G_4$	$\frac{+(\Lambda_1 + 3\Lambda_2)}{+(\Gamma_1 - 2\Gamma_2 + \Gamma_3 - \Gamma_4)}$	9.66
$2\sqrt{3}A(\Xi^0 \rightarrow \Lambda^0 \pi^0)$	$\frac{1}{2}B_1 + \frac{3}{2}B_2$	$\frac{-D_1 + D_4 - E_1 + E_4}{-G_1 + 2G_2 - G_3 + G_4}$	$\frac{-(\Lambda_1 + 3\Lambda_2)}{-(\Gamma_1 - 2\Gamma_2 + \Gamma_3 - \Gamma_4)}$	15.24

$$\begin{aligned}
\mathcal{B}(\Lambda^0 \rightarrow p\pi^-) &= (63.9 \pm 0.5) \times 10^{-2}, \\
\mathcal{B}(\Lambda^0 \rightarrow n\pi^0) &= (35.8 \pm 0.5) \times 10^{-2}, \\
\mathcal{B}(\Xi^- \rightarrow \Lambda^0 \pi^-) &= (99.887 \pm 0.035) \times 10^{-2}, \\
\mathcal{B}(\Xi^0 \rightarrow \Lambda^0 \pi^0) &= (99.524 \pm 0.012) \times 10^{-2}.
\end{aligned} \tag{24}$$

For  $\Sigma^0 \rightarrow p\pi^-, n\pi^0$  decays, which have not been measured yet, we may get the branching ratios in terms of the isospin relations [28]

$$\begin{aligned}
\mathcal{B}(\Sigma^0 \rightarrow p\pi^-) &= (4.82 \pm 0.50) \times 10^{-10}, \\
\mathcal{B}(\Sigma^0 \rightarrow n\pi^0) &= (2.41 \pm 0.26) \times 10^{-10}.
\end{aligned} \tag{25}$$

These measured branching ratios and obtained branching ratios from the isospin relations will help us to understand decay amplitudes of the tree diagrams and W-exchange diagrams. Using the central values in Eqs. (24-25) and the relation between the branching ratio and the moduli of the decay amplitudes in Eq. (8), one can backward obtain the ratios between the different moduli of decay amplitudes, which are given in the last column of Tab. V. Noted that we obtain the ratio by using  $|A(\Sigma^- \rightarrow n\pi^-)|$  as a unit, in which we including the coefficients in front of the amplitudes in the first column of Tab. V. For an example, in the second line and the last column of Tab. V, and the ratio 2.02 is obtained by using  $\frac{\sqrt{2}|A(\Sigma^+ \rightarrow p\pi^0)|}{|A(\Sigma^- \rightarrow n\pi^-)|}$ , which is also equal to  $\frac{|-B_2+D_2+E_2-E_3-F_2-G_2+2\Lambda_2-\Gamma_2|}{|-A_2+G_2-G_3-2\Lambda_2+\Gamma_2-\Gamma_3|}$ . After ignoring the penguin contributions since they are small, we have the following remarks for Tab. V.

- As shown in the third line, there is no tree diagram contribution to  $\Sigma^+ \rightarrow n\pi^+$  decay, nevertheless  $|A(\Sigma^+ \rightarrow n\pi^+)|$  may compare with others. So the W-exchange contributions can be as large as some tree diagram contributions.
- For the tree diagram amplitudes shown in Fig. 2 (a-b),  $A_i \propto C_2 + C_1/N_C \approx 1.153$  and  $B_i \propto C_1 + C_2/N_C \approx -0.171$ , *i.e.*,  $B_i$  are suppressed by the color-flavor factor. Comparing  $\sqrt{6}|A(\Lambda^0 \rightarrow p\pi^-)|$  with  $2\sqrt{3}|A(\Lambda^0 \rightarrow n\pi^0)|$  or comparing  $\sqrt{6}|A(\Xi^- \rightarrow \Lambda^0 \pi^-)|$  with  $2\sqrt{3}|A(\Xi^0 \rightarrow \Lambda^0 \pi^0)|$ , the formers included  $A_i$  are smaller than the latter included  $B_i$ , so the W-exchange diagrams give large and even dominant contribution to relevant decay amplitudes.

## IV. SUMMARY

In this work, we have analyzed the two-body nonleptonic decays of light baryon octet and decuplet by using the topological diagram approach to test the SU(3) flavor symmetry. Comparing with the IRA, the TPA is more intuitive and gives a better understanding of dynamics. Our main results can be summarized as follows:

- $T_{10} \rightarrow T_8 P_8$ : The TPA and the IRA can match in  $T_{10} \rightarrow T_8 P_8$  weak decays. We can predict all relevant decay branching ratios by using the TPA and also with the help of the IRA. Nevertheless, all branching ratios of relevant  $\Xi^{*0,-}$  and  $\Sigma^{*-}$  decays are very small since their lifetimes are small.
- $T_{10} \rightarrow T'_{10} P_8$ : We can obtain some amplitude relations and the ratios of the branching ratios by using the TPA and the SU(3) IRA, and then we obtain that  $\mathcal{B}(\Xi^{*0} \rightarrow \Sigma^{*+} \pi^-) < 2.1 \times 10^{-15}$  and  $\mathcal{B}(\Xi^{*-} \rightarrow \Sigma^{*0} \pi^-) < 1.5 \times 10^{-15}$  by using the experimental upper limit of  $\mathcal{B}(\Omega^- \rightarrow \Xi^{*0} \pi^-)$ .

- $T_8 \rightarrow T'_8 P_8$ : Since both initial state  $T_8$  and final state  $T'_8$  are all not fully symmetric or antisymmetric in flavor space, these decays are quite complex in the theory. Using some experiential branching ratios and other branching ratios obtained from the isospin relations, we analyze the contribution size of the tree diagrams and the W-exchange diagrams, and we find that the W-exchange diagrams give large and even dominant contribution to some decays.

All results in this work can be used to test the TPA in two-body nonleptonic decays of light baryons by BESIII, LHCb and the future experiments.

## ACKNOWLEDGEMENTS

The work was supported by the National Natural Science Foundation of China (Contract No. 11675137) and the Key Scientific Research Projects of Colleges and Universities in Hanan Province (Contract No. 18A140029).

## References

- 
- [1] M. Tanabashi et al. (Particle Data Group), Phys. Rev. D **98**, 030001 (2018).
  - [2] H. B. Li, Front. Phys. (Beijing) **12**, no. 5, 121301 (2017) [arXiv:1612.01775 [hep-ex]].
  - [3] I. I. Bigi, X. W. Kang and H. B. Li, Chin. Phys. C **42**, no. 1, 013101 (2018)
  - [4] D. M. Asner *et al.*, Int. J. Mod. Phys. A **24**, S1 (2009) [arXiv:0809.1869 [hep-ex]].
  - [5] M. Ablikim *et al.* [BESIII Collaboration], Nature Physics (2019), <https://doi.org/10.1038/s41567-019-0494-8>.
  - [6] R. Aaij *et al.* [LHCb Collaboration], Phys. Rev. Lett. **120**, no. 22, 221803 (2018) [arXiv:1712.08606 [hep-ex]].
  - [7] A. A. Alves Junior *et al.*, JHEP **1905**, 048 (2019), [arXiv:1808.03477 [hep-ex]].
  - [8] S. Weinberg, J. Phys. Conf. Ser. **196**, 012002 (2009).
  - [9] N. Severijns, M. Beck and O. Naviliat-Cuncic, Rev. Mod. Phys. **78**, 991 (2006) [nucl-ex/0605029].
  - [10] N. Cabibbo, Phys. Rev. Lett. **10**, 531 (1963).
  - [11] V. Cirigliano, M. Gonzalez-Alonso and M. L. Graesser, JHEP **1302**, 046 (2013) [arXiv:1210.4553 [hep-ph]].
  - [12] H. M. Chang, M. Gonzalez-Alonso and J. Martin Camalich, Phys. Rev. Lett. **114**, no. 16, 161802 (2015) [arXiv:1412.8484 [hep-ph]].
  - [13] G. Altarelli, N. Cabibbo and L. Maiani, Phys. Lett. **57B**, 277 (1975).
  - [14] M. J. Savage and R. P. Springer, Phys. Rev. D **42**, 1527 (1990).
  - [15] M. J. Savage, Phys. Lett. B **257**, 414 (1991).
  - [16] R. Arora, G. K. Sidana and M. P. Khanna, Phys. Rev. D **45**, 4121 (1992).
  - [17] D. S. Du and D. X. Zhang, Phys. Rev. D **50**, 2058 (1994).
  - [18] J. G. Korner, M. Kramer and D. Pirjol, Prog. Part. Nucl. Phys. **33**, 787 (1994) [hep-ph/9406359].
  - [19] D. A. Egolf, R. P. Springer and J. Urban, Phys. Rev. D **68**, 013003 (2003) [hep-ph/0211360].
  - [20] Y. K. Hsiao and C. Q. Geng, Phys. Rev. D **91**, no. 11, 116007 (2015) [arXiv:1412.1899 [hep-ph]].

- [21] M. Gronau and J. L. Rosner, Phys. Rev. D **89**, no. 3, 037501 (2014) Erratum: [Phys. Rev. D **91**, no. 11, 119902 (2015)] [arXiv:1312.5730 [hep-ph]].
- [22] M. He, X. G. He and G. N. Li, Phys. Rev. D **92**, no. 3, 036010 (2015) [arXiv:1507.07990 [hep-ph]].
- [23] X. G. He and G. N. Li, Phys. Lett. B **750**, 82 (2015) [arXiv:1501.00646 [hep-ph]].
- [24] Y. K. Hsiao, C. F. Chang and X. G. He, Phys. Rev. D **93**, no. 11, 114002 (2016) [arXiv:1512.09223 [hep-ph]].
- [25] M. Gronau and J. L. Rosner, Phys. Rev. D **93**, no. 3, 034020 (2016) [arXiv:1512.06700 [hep-ph]].
- [26] C. D. L, W. Wang and F. S. Yu, Phys. Rev. D **93**, no. 5, 056008 (2016) [arXiv:1601.04241 [hep-ph]].
- [27] C. Q. Geng, Y. K. Hsiao, C. W. Liu and T. H. Tsai, Phys. Rev. D **99**, no. 7, 073003 (2019) doi:10.1103/PhysRevD.99.073003 [arXiv:1810.01079 [hep-ph]].
- [28] R. M. Wang, M. Z. Yang, H. B. Li and X. D. Cheng, Phys. Rev. D **100**, no. 7, 076008 (2019) [arXiv:1906.08413 [hep-ph]].
- [29] A. Dery, M. Ghosh, Y. Grossman and S. Schacht, arXiv:2001.05397 [hep-ph].
- [30] D. Zeppenfeld, Z. Phys. C **8**, 77 (1981).
- [31] L. L. Chau and H. Y. Cheng, Phys. Rev. Lett. **56**, 1655 (1986).
- [32] L. L. Chau and H. Y. Cheng, Phys. Rev. D **36**, 137 (1987) Addendum: [Phys. Rev. D **39**, 2788 (1989)].
- [33] M. J. Savage and M. B. Wise, Phys. Rev. D **39**, 3346 (1989) Erratum: [Phys. Rev. D **40**, 3127 (1989)].
- [34] M. Gronau, O. F. Hernandez, D. London and J. L. Rosner, Phys. Rev. D **50**, 4529 (1994) [hep-ph/9404283].
- [35] M. Gronau, O. F. Hernandez, D. London and J. L. Rosner, Phys. Rev. D **52**, 6374 (1995) [hep-ph/9504327].
- [36] L. L. Chau, H. Y. Cheng, W. K. Sze, H. Yao and B. Tseng, Phys. Rev. D **43**, 2176 (1991) Erratum: [Phys. Rev. D **58**, 019902 (1998)].
- [37] H. Y. Cheng, C. W. Chiang and A. L. Kuo, Phys. Rev. D **91**, no. 1, 014011 (2015) [arXiv:1409.5026 [hep-ph]].
- [38] C. Wang, Q. A. Zhang, Y. Li and C. D. Lu, Eur. Phys. J. C **77**, no. 5, 333 (2017) [arXiv:1701.01300 [hep-ph]].
- [39] S. H. Zhou, Q. A. Zhang, W. R. Lyu and C. D. L, Eur. Phys. J. C **77**, no. 2, 125 (2017) [arXiv:1608.02819 [hep-ph]].
- [40] C. W. Chiang and Y. F. Zhou, JHEP **0612**, 027 (2006) [hep-ph/0609128].
- [41] S. H. Zhou, Y. B. Wei, Q. Qin, Y. Li, F. S. Yu and C. D. Lu, Phys. Rev. D **92**, no. 9, 094016 (2015) [arXiv:1509.04060 [hep-ph]].
- [42] C. W. Chiang and Y. F. Zhou, JHEP **0903**, 055 (2009) [arXiv:0809.0841 [hep-ph]].
- [43] S. Mller, U. Nierste and S. Schacht, Phys. Rev. D **92**, no. 1, 014004 (2015) [arXiv:1503.06759 [hep-ph]].
- [44] X. G. He and W. Wang, Chin. Phys. C **42**, no. 10, 103108 (2018) [arXiv:1803.04227 [hep-ph]].
- [45] G. Buchalla, A. J. Buras and M. E. Lautenbacher, Rev. Mod. Phys. **68**, 1125 (1996) [hep-ph/9512380].
- [46] X. G. He, Y. J. Shi and W. Wang, arXiv:1811.03480 [hep-ph].
- [47] J. G. Körner, Nucl. Phys. B **25**, 282 (1971).
- [48] J. C. Pati and C. H. Woo, Phys. Rev. D **3**, 2920 (1971).